






## Article

# Feasibility of Using Sugar Cane Bagasse Ash in Partial Replacement of Portland Cement Clinker

Sâmara França <sup>1</sup>, Leila Nóbrega Sousa <sup>2</sup>, Sérgio Luiz Costa Saraiva <sup>2</sup>, Maria Cecília Novaes Firmo Ferreira <sup>2</sup>, Marcos Vinício de Moura Solar Silva <sup>3</sup>, Romero César Gomes <sup>4</sup>, Conrado de Souza Rodrigues <sup>1</sup>, Maria Teresa Paulino Aguilár <sup>5</sup> and Augusto Cesar da Silva Bezerra <sup>1,2,\*</sup>

<sup>1</sup> Department of Civil Engineering, Federal Center for Technological Education of Minas Gerais, Belo Horizonte 30421-169, Brazil

<sup>2</sup> Department of Transport Engineering, Federal Center for Technological Education of Minas Gerais, Belo Horizonte 30421-169, Brazil

<sup>3</sup> Energy Company of Minas Gerais, Belo Horizonte 30190-131, Brazil

<sup>4</sup> Núcleo de Geotecnia, Federal University of Ouro Preto, Ouro Preto 35400-000, Brazil

<sup>5</sup> Department of Materials and Construction Engineering, Federal University of Minas Gerais, Belo Horizonte 31270-901, Brazil

\* Correspondence: augustobezerra@cefetmg.br; Tel.: +55-319-9388-6780

**Abstract:** This work presents a technical and economic study using sugar cane bagasse ash (SCBA) to partially replace Portland cement clinker. To evaluate the technical viability, the replacement rates of 10, 20, and 30% of Portland cement were used in the experiments. The ashes used were in the following conditions: (i) as collected (AC), (ii) ground (G), and (iii) re-burnt and ground (RG). Three composition parameters were used in the mortar mix procedures: (i) mix with water factor/fixed binder in volume, (ii) mix with water factor/fixed binder in weight, and (iii) mix with the fixed flow. After the technical feasibility analysis, the benefit of the substitutions and an analysis of the relationship between cement consumption and the acquired compressive strength, correlating with possible economic costs, were discussed. SCBA AC was not suitable for the partial replacement of Portland cement clinker. SCBA G presented a satisfactory performance and SCBA RG was the ash that presented the best performance in the partial replacement of Portland cement clinker. For the same levels of compressive strength, the consumption of Portland cement per cubic meter of concrete reduced; from this, the cost of concrete and mortar could be reduced by 8%, with the ash having the same value as cement. Furthermore, the use of SCBA RG at 30% inhibited the alkali–silica reaction (ASR) in concretes with a reactive basalt and quartzite aggregate. SCBA G (20 and 30%) and SCBA RG (10 and 20%) inhibited the ASR in concretes with a reactive basalt aggregate and reduced the expandability in concretes with a reactive quartzite aggregate. Another point to highlight was the durability shown by the cements with SCBA, which, 900 days after the accelerated test of expansion by the alkali–aggregate reaction, maintained high levels of flexural strength when compared to the results obtained before the accelerated test of expansion. The present work concluded that using sugar cane bagasse ash to replace Portland cement is feasible from a technical, environmental, and economic perspective.

**Keywords:** sugar cane bagasse ash; supplementary cement material; eco-friendly Portland cement; sustainability



**Citation:** França, S.; Sousa, L.N.; Saraiva, S.L.C.; Ferreira, M.C.N.F.; Silva, M.V.d.M.S.; Gomes, R.C.; Rodrigues, C.d.S.; Aguilár, M.T.P.; Bezerra, A.C.d.S. Feasibility of Using Sugar Cane Bagasse Ash in Partial Replacement of Portland Cement Clinker. *Buildings* **2023**, *13*, 843. <https://doi.org/10.3390/buildings13040843>

Academic Editor: Elena Ferretti

Received: 30 January 2023

Revised: 17 March 2023

Accepted: 20 March 2023

Published: 23 March 2023



**Copyright:** © 2023 by the authors. Licensee MDPI, Basel, Switzerland. This article is an open access article distributed under the terms and conditions of the Creative Commons Attribution (CC BY) license (<https://creativecommons.org/licenses/by/4.0/>).

## 1. Introduction

Portland cement is the most significant manufactured product on Earth by weight. Combined with water and aggregates, it forms cement-based materials (e.g., concrete). It is the second-most-used material on the planet after water [1]. In 2021, 4.4 billion tons of Portland cement were produced worldwide, with 3.7 billion tons of Portland clinker. In 2021, Brazil produced approximately 55 million tons of cement [2].

The manufacture of 1 ton of cement would produce approximately 1 ton of CO<sub>2</sub> [3], which can be a problem due to its high consumption. Supplementary cement materials (SCM) are often employed to reduce the environmental impact of cement [4,5]. Scrivener et al. say cement contains only about 20% of SCMs substituting Portland cement clinker [1]. There are several SCMs around the world, including: fine limestone [6,7], granulated blast-furnace slags (GBFS) [8–10], coal fly ashes (FA) [11], silica fume [11], calcined clays [12,13], rice husk ash [14], sugar cane bagasse ash [14], and tailings [15–17]. Brazilian standards allow up to 75% of SCMs, in some cases, such as GBFS [18]. However, there is not enough slag generation in Brazil to supply Portland cement production. It is estimated that the global iron slag output in 2021 was 340 to 410 million tons [2], i.e., 10% of Portland clinker production, and not all of the products produced are suitable for producing cement. The possibility of using waste to replace traditional Portland cement-based construction materials promotes the mitigation of environmental impacts [10,19]. It contributes to the fulfillment of Sustainable Development Goal 12 (SDG-12: Responsible Consumption and Production), related to substantially reducing waste generation through prevention, reduction, recycling, and reuse [20]. In addition, when added to Portland cement, supplementary cementitious materials improve the properties of mortars and concretes, such as increased strength [21,22], reduction of Portland cement consumption [23–26], reduced hydration heat [5,27], reduced carbonation [5,27], increased chemical resistance and durability [28], and increased fire resistance [11].

Scrivener et al. believe that GBFS, FA, waste glass, and silica fume cannot meet the demand for SCMs to produce cement, and claim that ash from agricultural production would not be enough either [1]. Among the residues from agrarian production used as SCM is sugar cane bagasse ash (SCBA) generated from burning to produce bioelectricity. Currently, the SCBA is not being used in the United States or Europe and is presently being landfilled [4]. However, in countries such as Brazil, India, and China that have high sugar cane production [29], SCBAs are not intended to fertilize crops, so these ashes with adequate characteristics can be used as SCMs. A Portland cement clinker partial replacement with SCBA can improve the composite's mechanical properties and support a more sustainable material [30]. It is essential to emphasise that, even as the bagasse combustion releases CO<sub>2</sub>, the CO<sub>2</sub> emission total is basically zero when the full cycle is deemed because photosynthesis restores the burned biomass in the next sugar cane harvest [30,31].

Due to the restricted use of SCBA as SCM, data regarding its application as a substitute for Portland cement in concrete are not widely acknowledged [4]; however, there are several studies on the mechanical behavior of compounds from Portland cement with a partial replacement by SCBA and the mechanical and thermal treatment of SCBA [31–33]. However, no reports on the technical feasibility combined with economic and environmental feasibility were found. This study aimed to evaluate the processing of SCBA to replace Portland cement clinker in the production of mortars and concrete. Still on the objective of the study, it is expected to evaluate the influence of ash processing in the production of mortars in different dosages, in the physical and mechanical properties, in the durability, and in the economic viability.

## 2. Materials and Methods

To carry out the present work, SCBA was collected in an industry in Alto Paranaíba and Triângulo Mineiro's mesoregion in the state of Minas Gerais, Brazil. Cogeneration boilers from sugar and alcohol plants generally have an electrostatic precipitator to collect the flying SCBA and a hopper to collect the ashes that are deposited on the bottom [34]; the SCBA used in this work was collected by the electrostatic precipitator. The SCBA was kiln-dried at  $100 \pm 5$  °C until dough consistency and was processed by grinding and blasting. The grinding was carried out in a planetary mill in 500 mL vessels and 16 zirconia oxide spheres with a diameter of 10 mm for 10 min at 300 rpm. Grinding was performed every 2 min up to 12 min, and the best grinding occurred in 10 min [35,36]. The adequate

burning of the bagasse is at a temperature of 600 °C with a burning level of 3 h and a heating rate of 10 °C/min, and the bagasse was pre-burned at 350 °C for 3 h [37]. As the bagasse ash was already used in this work, the pre-firing step was suppressed, with only the ash burning in an electric resistance oven with forced air circulation.

The characterization tests were selected to characterize the ashes, mainly regarding the chemical composition, morphology, and particle size. After processing, the 3 types of SCBA were characterized, the SCBA as it was collected in the industry (SCBA AC), the ground SCBA (SCBA G), and the reburning and ground SCBA (SCBA RG). SCBA AC, G, and RG were characterized by images obtained by conventional photographic equipment, X-ray fluorescence spectrometry (XRF), X-ray diffraction (XRD), scanning electron microscopy (SEM), loss on ignition (LOI) [38], laser particle size (LG), dry bulk density, pozzolanic index with Portland cement [39], and pozzolanicity using the modified Chapelle method [40].

The SEM examinations were performed with magnification from 15 to 30,000 times variable pressure, BSE (backscattered electron) detector, and an accelerating voltage of 15 kV [30,36,41,42]. The XRD measurements were made with continuous scanning mode and a  $2\theta$  of 5° that changed until 90°, at 2° every minute, utilizing a copper X-ray tube with 40 kV accelerating voltage and a 30 mA current [17,30,42,43]. XRF was performed with atmospheric air and a collimator of 10 mm [30,42]. The LG was performed in water, not including a dispersive liquid, with ultrasounds utilized for one minute and an obscuration of 10% [30,42].

The pozzolanicity of the SCBA was evaluated according to NBR 5752 [39] and NBR 15895 [40]. The NBR 5752 [39] prescribes for two mortars to be prepared: (i) mortar Type I should contain Portland cement only; and (ii) mortar Type II has 35% of the total volume of cement replaced by the pozzolanic material. Three 50 mm × 100 mm cylindrical specimens were manufactured for each type of mortar. The initial and final setting times of Portland cement with SCBA were determined according to NBR NM 65 [44].

The ashes were used to substitute reference Portland cement in the percentages of 10, 20, and 30% in volume. For produced mortar, 624 g of Portland cement and 1872 g of Brazilian standard sand were used [45], i.e., proportion of 1:3 (cement:sand). The sand was divided into four granulometric fractions per dosage [46]. The binder used was reference Portland cement, in the Brazilian standard, called high initial strength cement or V-type cement, produced with Portland cement clinker (~95 wt%) and gypsum (~5 wt%), trying to represent a cement not including additions [18], comparable to CEM I of the European standard EN 197-1 [47], which permits until 5% of minor additional constituents.

Three dosing conditions were used for the production of mortars: (i) mix with constant water/binder ratio in volume, that is, constant water consumption (300 mL), which represents a constant water/binder ratio in volume, where the weight of the binder is the sum of the weight of Portland cement and SCBA; (ii) constant water/binder ratio in weight ( $w/b = 0.48$ ); (iii) fixed workability (water/ binder ratio in variable weight and volume) represented by the opening diameter of the mortar of 225 mm in the flow table test. For each proportion, 5 cylindrical specimens of 50 mm diameter by 100 mm height were molded for the compression test, and 3 prismatic specimens of 40 mm × 40 mm × 160 mm for flexural strength test. For the compressive strength test, the cylindrical specimens had their base and top surfaces rectified. Compressive strength was determined at 3, 7, 28, and 91 days; and flexural strength was determined at 28 days. An EMIC DL 30000 universal testing machine and the software TESC and Vmaq were used for the mechanical tests, with an increasing stress rate of 0.25 MPa/s for the compression test and load rate of 50 N/s for the flexural test [17,45,48].

The water absorption and dry bulk density were performed according to NBR 9778 [49]. For this, the weights of the oven-dry, saturated surface-dry sample in air, and saturated test samples immersed in water were measured. The water absorption and dry bulk density were calculated according to the following equations:

$$\text{Water absorption}(\%) = \frac{m_{\text{sat}} - m_d}{m_d} 100 \quad (1)$$

$$\text{Bulk density, dry} \left( \frac{\text{g}}{\text{cm}^3} \right) = \frac{m_d}{m_{sat} - m_i} \rho \quad (2)$$

where  $m_{sat}$  is the saturated weight of surface-dry sample in air (g),  $m_d$  is the weight of oven-dried sample in air (g),  $m_i$  is the saturated weight immersed in water (g), and  $\rho$  is the density of water = 1 g/cm<sup>3</sup>.

A durability parameter chosen to evaluate mortars with SCBA was the alkali–silica reaction (ASR) expandability. The efficiency of SCBA AC preventing expansion due to ASR was evaluated by the accelerated method of expandability with mortar bars made with two potentially reactive aggregates [50,51].

To choose the potentially reactive aggregates, 3 aggregates were tested: (i) Brazilian standard sand [46]; (ii) quartzite remaining from the construction of the Jaguara Hydroelectric Plant (Sacramento City, Minas Gerais, Brazil); and (iii) basalt remaining from the construction of the Nova Ponte Hydroelectric Plant (Nova Ponte City, Minas Gerais, Brazil). The quartzite and basalt deposits can be seen in Figures 1 and 2. The choice of Brazilian standard sand was due to the possibility of reproducibility and repeatability of the tests. With natural river sand, the reproducibility and repeatability of the tests would be impaired.



Figure 1. Quartzite deposit.



Figure 2. Basalt deposit.

Quartzite and basalt were collected in coarse aggregate size (Figure 3). For the mortar prism accelerated expandability test (detailed below), the quartzite and basalt fragments had to be crushed and sieved to meet the granulometric requirements [50,52]. Figures 4–6 show Brazilian standard sand, quartzite sand, and basalt sand.

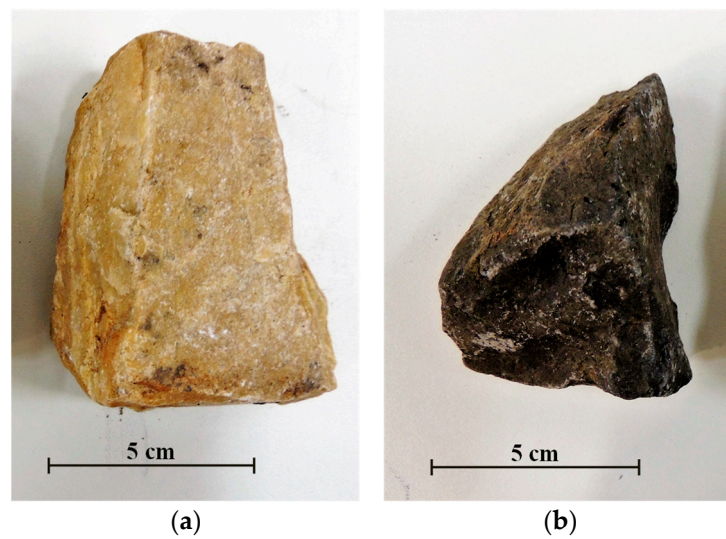


Figure 3. Quartzite rock fragment (a) and basalt rock fragment (b).

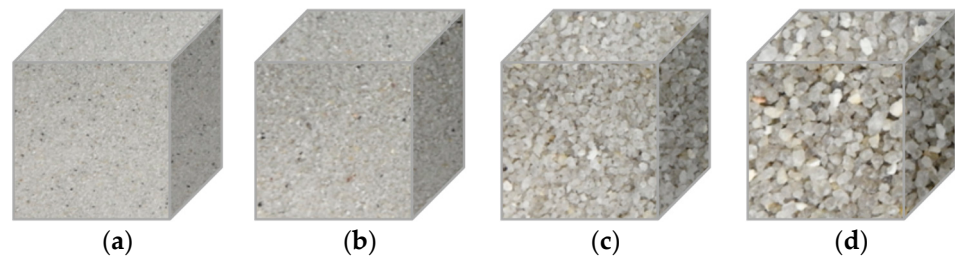


Figure 4. Brazilian standard sand: (a) #0.15 mm; (b) #0.30 mm; (c) #0.60 mm; and (d) #1.20 mm.

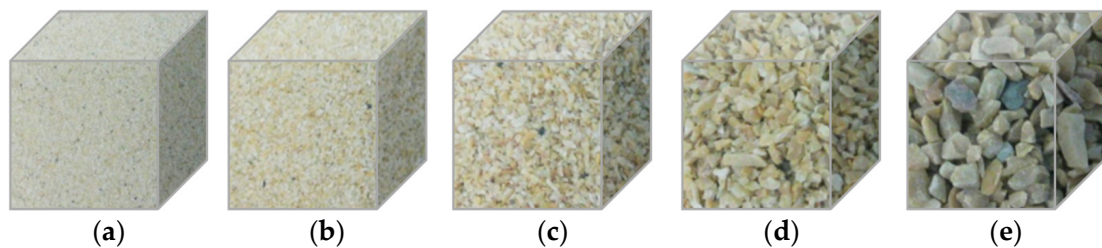


Figure 5. Quartzite sand: (a) #0.15 mm; (b) #0.30 mm; (c) #0.60 mm; (d) #1.20 mm; and (e) #2.40 mm.

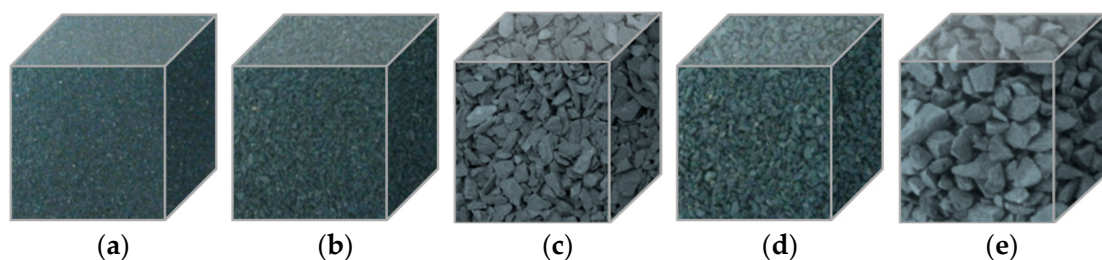
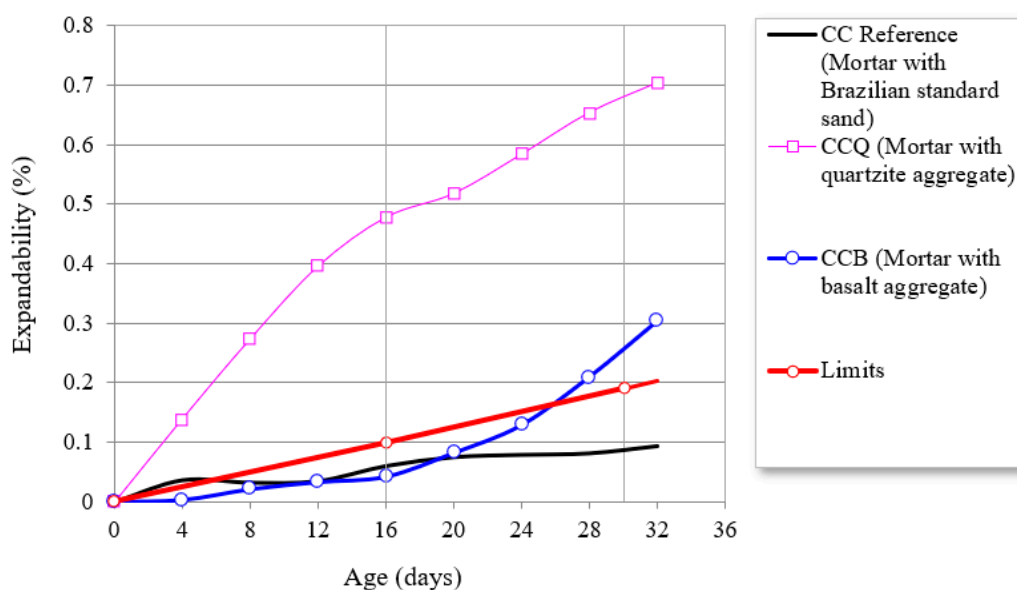


Figure 6. Basalt sand: (a) #0.15 mm; (b) #0.30 mm; (c) #0.60 mm; (d) #1.20 mm; and (e) #2.40 mm.

The preliminary test to evaluate the reactivity of the aggregate indicated that the Brazilian standard sand is not reactive by ASR expandability. Differently, quartzite and basalt are reactive by ASR (Figure 7). As the objective is to evaluate the inhibitory potential of SCBA in combating ASR, only quartzite and basalt were used for this evaluation.



**Figure 7.** Comparison between the expandability of mortars developed with Brazilian standard sand, quartzite, and basalt aggregates.

To continue the tests, three  $25 \times 25 \times 285$  mm prismatic specimens were molded for each proportion of materials, and they remained 24 h in the metal molds with a glass plate over the molds. The laboratory's temperature and humidity were controlled during molding at  $24 \pm 2$  °C and above 50%, respectively. After 24 h, the specimens were demolded and placed in a thermal tank regulated at  $80 \pm 2$  °C, where they were submerged in distilled water for 24 h. After 24 h, the specimens were retired from the water tank, and length readings were taken. After the reading, the specimens were placed into a thermal tank regulated at 80 °C, where they were immersed in sodium hydroxide solution in the concentration predicted by the norm until the date of 32 days, and readings of expandability were performed every 4 days. After the expandability readings, the specimens were dried in an oven and stored for 900 days, and tested for flexural tensile strength. The mortars for the expandability test were developed with a 1:2.25 line (Table 1), and artificial sand was produced by crushing and granulometric separation of basalt and quartzite. Mortars also had specimens molded to assess flexural strength before the expandability tests.

**Table 1.** Proportions of materials used in mortars.

CC = Cementitious Composite B = Basalt Q = Quartzite	Replacement (%)	Consumption of Materials (g)							Water
		Cement	Ash	Fine Aggregate (Basalt or Quartzite)					
				Particle Size					
				0.15 mm	0.30 mm	0.60 mm	1.20 mm	2.40 mm	
CCB or CCQ	0	440.0	0.0	148.5	247.5	247.5	247.5	99.0	206.8
CCB SCBA G or CCQ SCBA G	10	396.0	28.0	148.5	247.5	247.5	247.5	99.0	206.8
	20	352.0	56.0	148.5	247.5	247.5	247.5	99.0	206.8
	30	308.0	84.0	148.5	247.5	247.5	247.5	99.0	206.8
CCB SCBA RG or CCQ SCBA RG	10	396.0	37.6	148.5	247.5	247.5	247.5	99.0	206.8
	20	352.0	75.2	148.5	247.5	247.5	247.5	99.0	206.8
	30	308.0	112.8	148.5	247.5	247.5	247.5	99.0	206.8

### 3. Results

In Figure 8, it is possible to observe images of SCBA, showing the difference in color and texture between SCBA AC, G, R, and RG. The SCBA processing has to alter the visual appearance and alter the density. The SCBA AC, M, and RG showed a density of 1.720, 1.977, and 2.653 g/cm<sup>3</sup>.

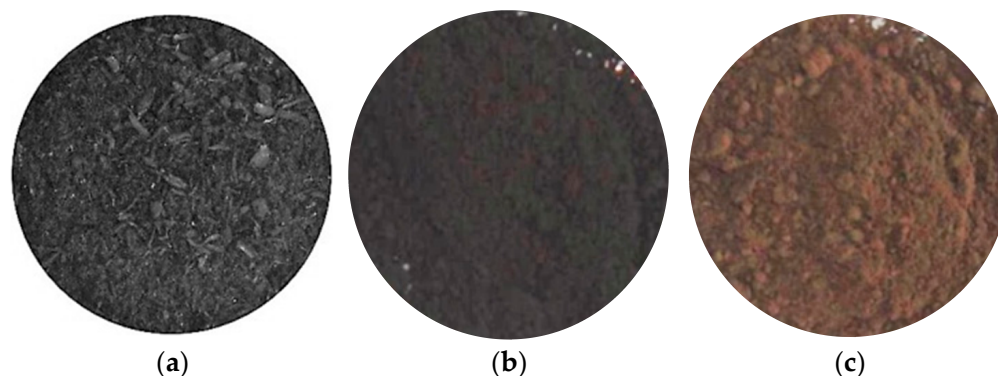
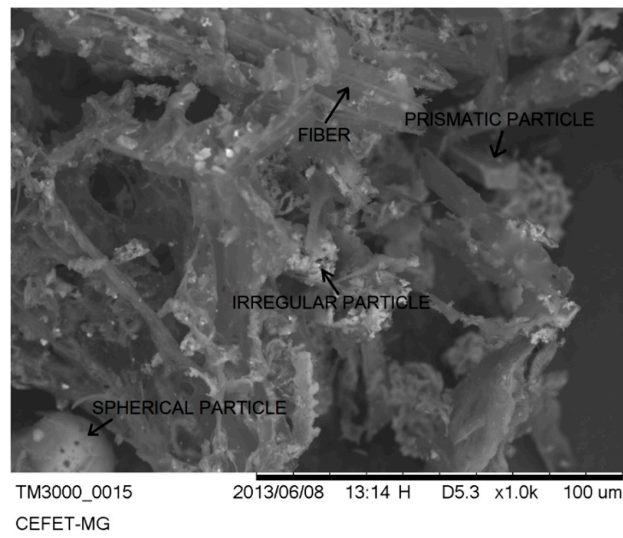


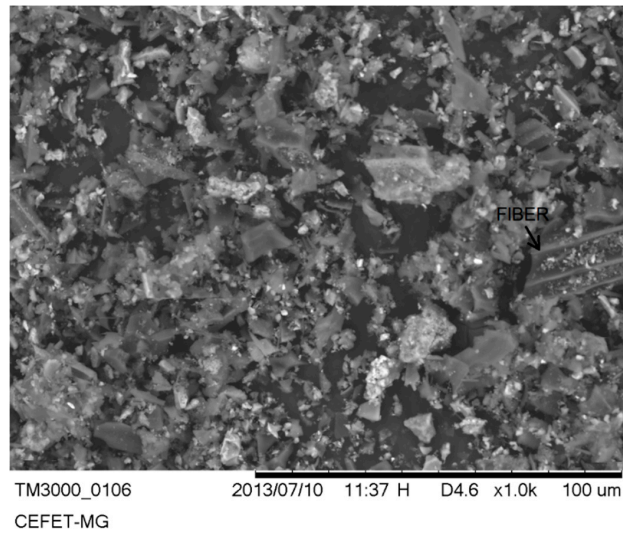
**Figure 8.** SCBA images: (a) SCBA AC; (b) SCBA G; and (c) SCBA RG.

In Figure 9, it is possible to observe images of SCBA obtained by SEM at the same magnification scale. In Figure 9a, it is possible to observe that SCBA AC presents a fibrous, spherical, and prismatic structure, as shown in the lower-left corner of the image as a spherical particle [30,53–57]. In Figure 9b, it can be seen that SCBA G has a reduced particle size. The fibrous structures have been comminuted; however, it is still possible to identify the fiber's presence in the reduced size example, on the right side of the image. In Figure 9c, it is not possible to verify the fiber's existence in the SCBA RG.

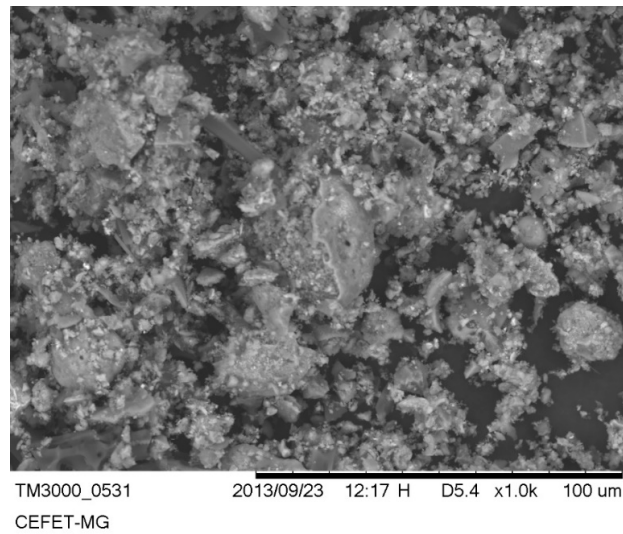
The SCBA's chemical composition as a function of the principal oxides by XRF is shown in Table 2. SCBA presented SiO<sub>2</sub> as the principal oxide, followed by Al<sub>2</sub>O<sub>3</sub> and Fe<sub>2</sub>O<sub>3</sub> [58]. The sum of these three oxides for SCBA G and RG is 41.75 and 80.26%, respectively, in agreement with previous results [32,37]. Comparing the values obtained for Na<sub>2</sub>O and K<sub>2</sub>O, it is noticed that SCBA G and RG present higher values than cement, indicating that the replacement of cement by ash will increase the system's alkalis, which may contribute to the occurrence of an alkali-aggregated reaction. Table 3 shows the particle diameters of SCBA G and SCBA RG obtained by laser granulometry. The results found are consistent with the literature [59–61]. It is noticed that SCBA RG presented smaller dimensions, leading to better performances in cementitious composites [17,55,62]. SCBA G and SCBA RG present smaller particle sizes than the reference Portland cement and with  $D_{\text{average}}$  of the particles smaller than 13.53  $\mu\text{m}$  for SCBA G and 11.88  $\mu\text{m}$  for SCBA RG. Particle size distribution showed that the samples satisfy the ASTM C618 [38] fineness criterion for coal fly ash and raw or calcined natural pozzolan, with less than 34% of the material retained on a 0.045 mm or 45  $\mu\text{m}$  sieve. Brazilian Standard NBR 12653 [63] prescribes that the material, to be pozzolanic, must be presented with less than 20% of the material retained on a 0.045 mm sieve. The reference Portland cement's granulometry is also presented, and we can see the proximity of the results between the binders [17]. The results of the chemical analysis of SCBA AC were not presented, as the grinding process is necessary to perform the analysis. The granulometry result was also not presented because the granulometry presented by SCBA AC was higher than the limit of the equipment used for the determination by the laser diffraction technique. The re-burning significantly reduced the loss on ignition (LOI) of the SCBA [64].



(a)



(b)



(c)

Figure 9. SEM of SCBAs: (a) SCBA AC; (b) SCBA G; (c) SCBA RG.

**Table 2.** Chemical composition by XRF, particle density, and particle size distribution of the samples.

	Portland Cement	SCBA G	SCBA RG
Chemical composition by XRF (wt%)			
SiO <sub>2</sub>	6.8	21.1	40.5
Al <sub>2</sub> O <sub>3</sub>	4.9	13.0	24.8
Fe <sub>2</sub> O <sub>3</sub>	4.5	7.7	15.0
CaO	78.3	2.0	3.8
MgO	1.5	1.2	2.3
TiO <sub>2</sub>	0.2	2.3	4.4
P <sub>2</sub> O <sub>5</sub>	0.0	1.0	1.6
Na <sub>2</sub> O	0.1	0.2	0.4
K <sub>2</sub> O	0.4	2.2	3.7
MnO	0	0.1	0.1
LOI	3.4	49.2	3.3
Particle density (g/cm <sup>3</sup> )	3.106	1.977	2.653
Particle size distribution			
D <sub>10</sub> (μm)	2.46	2.12	1.39
D <sub>50</sub> (μm)	11.70	9.58	8.47
D <sub>90</sub> (μm)	27.50	32.29	28.62
D <sub>average</sub> (μm)	13.66	13.53	11.88

**Table 3.** Pozzolanic activity of SCBA.

Mortar	Flow (mm)	Water (g)	Compressive Strength (MPa)	Pozzolanic Activity (%)
Type I "A" (Portland cement)	225.0	162.7	43.08	100.0
Type II "B" (SCBA G 35%)	225.0	168.1	35.93	83.4
Type II "C" (SCBA RG 35%)	225.0	179.4	38.17	88.6

From the diffractograms of SCBA G and RG, it was possible to identify the peaks of crystallinity of quartz (Crystallography Open Database (COD) 9013321) [65], alumina (Crystallography Open Database (COD) 1528427) [66], and hematite (Crystallography Open Database (COD) 1011240) [67] (Figure 10). Thus, it can be said that part of the oxides of silicon, aluminum, and iron detected in XRF is presented in a crystalline form. The SiO<sub>2</sub> found in XRD is crystalline; however, SiO<sub>2</sub> can be crystalline or amorphous [30]. The detected quartz is mainly due to soil contamination [32,68]. The amorphous halo ( $2\theta = 20\text{--}30^\circ$ ) of the SCBA G diffractogram was higher due to the material with incomplete burning [32]. The re-burning was influential in the removal of organic material [69].

To evaluate the pozzolanicity of a material, a mortar with a 35% cement replacement (Type I) by the material must obtain at least 75% of the compressive strength of the mortar without replacement (Type II) [39]. Thus, the SCBA G and RG analyzed can be considered pozzolanic once, with an average compressive strength of 35.93 and 38.17 MPa, reaching 83.40 and 88.6% of the average compressive strength found for the samples prepared without the use of ash (average of 43.08 MPa), respectively (Table 3). For the same flow, the mortars with SCBA (B and C) demanded more water than the reference mortar (A), a trend in the use of SCBA [58]. According to NBR 15895 [40], Chapelle's test modified for SCBA G and RG indicates 361 and 382 mg/g of Ca(OH)<sub>2</sub> fixation, respectively. For samples to have pozzolanicity, they must be fixed with at least 330 mg of Ca(OH)<sub>2</sub>. In general, SCBA G and SCBA RG can be considered pozzolanic, as with SCBA studied by other authors [70]. Grinding and re-firing improved SCBA's pozzolanic activity [71].

The flow table, cement setting time, dry bulk density, and water absorption results of the mortars dosed with a trace with water/binder factor fixed in volume ( $w/b$  in equal volume 0.48) are presented in Table 4. The SCBA AC significantly reduced the workability of the mortars. SCBA G and RG reduced mortar workability [55,72,73], except SCBA G 30%. It is believed that the inclusion of SCBA AC mortar mixes increased both the viscosity

and yield stress, which caused a reduction in fluidity [74]. The mortar setting time did not significantly decrease with SCBA G and SCBA RG; the same cannot be said to start grouting with SCBA AC. The dry bulk density of sugar cane bagasse ash mortar is within the typical weight of mortar or concrete [75]. SCBA AC and SCBA G led to mortars with a lower dry bulk density and more excellent water absorption. SCBA RG led to denser mortars with less water absorption, except for SCBA RG 10%, which obtained slightly higher water absorption. The results obtained by mortars with SCBA RG may indicate the possibility of producing more durable concretes, mainly in reducing porosity indirectly assessed by reducing water absorption.

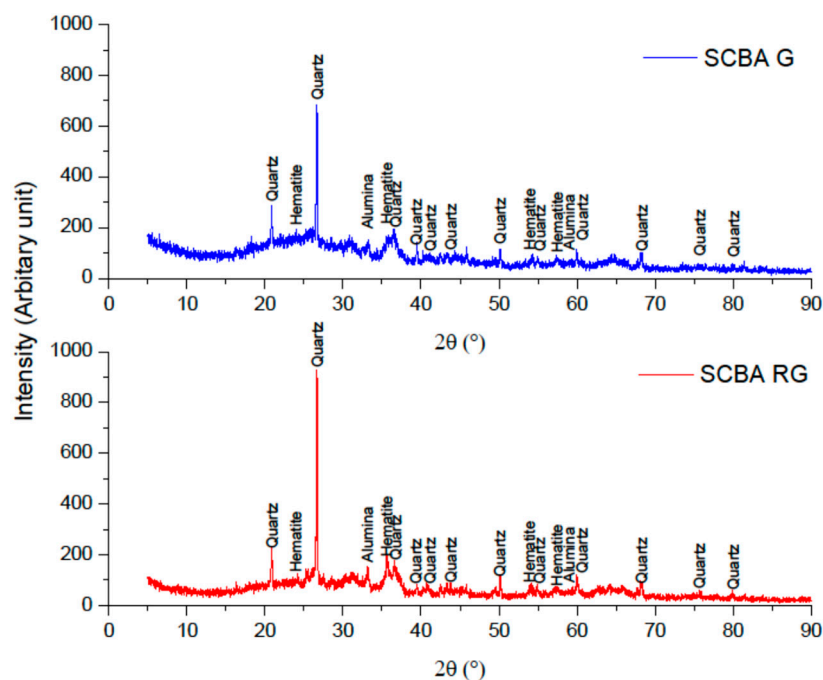


Figure 10. XRD of SCBAs.

Table 4. Flow, cement setting time, dry bulk density, and water absorption.

Addition	Substitution (%)	Flow (mm) <sup>1</sup>	Cement Setting Times (min) <sup>2</sup>		Dry Bulk Density (g/cm <sup>3</sup> ) <sup>1</sup>	Water Absorption (%) <sup>1</sup>
			Start	End		
CC Reference	0	172.5 (0.5) <sup>3</sup>	142	191	2.168 (0.003)	6.65 (0.08)
CC SCBA AC	10	Dry mix (Disaggregated)	139	183	2.156 (0.013)	7.12 (0.17)
	20	Dry mix (Disaggregated)	135	183	2.133 (0.007)	7.51 (0.25)
	30	Dry mix (Disaggregated)	129	181	2.129 (0.008)	7.72 (0.15)
CC SCBA G	10	168.0 (0.9)	146	196	2.162 (0.005)	7.03 (0.13)
	20	169.0 (0.0)	143	195	2.142 (0.006)	7.17 (0.14)
	30	176.0 (0.5)	141	191	2.141 (0.005)	6.90 (0.24)
CC SCBA RG	10	166.5 (0.9)	141	188	2.169 (0.010)	6.79 (0.47)
	20	166.5 (0.0)	143	191	2.171 (0.008)	6.24 (0.28)
	30	166.0 (0.0)	143	190	2.178 (0.006)	6.10 (0.14)

<sup>1</sup> Test performed in triplicate. <sup>2</sup> Test performed on a single sample. <sup>3</sup> Standard deviation in parentheses.

In Figure 11, it is possible to observe the results of the developed mortars' compressive strength. In general, mortar strength development was due to pozzolanic activity and physical effects [76]. SCBA AC caused a drop in strength, confirming the low viability of its use without any processing. On the other hand, the compressive strengths remained approximately constant when using SCBA G and SCBA RG in mortars with a fixed water/binder factor in volume. The behavior for mortars with a fixed water/binder factor in weight (Figure 12) remained the same trend as with the mix with a water/fixed binder factor in volume, with a drop in strength for SCBA AC. For mortars with a fixed flow factor, the preparation of mortars within natural ash proved impracticable due to the large amount of water involved in reaching the spread on the 225 mm flow table. The amount of water demanded the maintenance of the 225 mm spread on the flow table to be increased with the increase in ash (Figure 13). The reference mortar required 325.4 g of water for a standard dosing with 624 g of Portland cement and 1824 g of standardized sand. For dosages with the replacement of 10, 20, and 30% Portland cement by SCBA AC, the amount of water for maintaining workability was changed to 363.3, 377.6, and 383.1 g, respectively. For mortars with SCBA G 10, 20, and 30% and SCBA RG 10, 20, and 30%, water consumption was 338.9, 347.9, 361.1, 340.6, 351.4, and 357.5 g, respectively. It is noticed that mortars with SCBA RG, even when requiring more water to maintain workability, presented a compressive strength similar to the reference mortar. Thus, it is believed that using plasticizer additives in conjunction with SCBA RG can significantly optimize compressive strength.

The consumption of binder in a cubic meter of mortar divided by the compressive strength of the mortars with a fixed water/volume factor is shown in Table 5. It should be noted that the SCBA consumption per volume ( $\text{kg}/\text{m}^3$ ) is detached from the X axis to facilitate reading, but the vertical length of the gray bar represents the amount of ash per cubic meter of mortar. It is possible to observe that the lowest Portland cement clinker consumption was 8.31  $\text{kg}/\text{MPa}$  for the mortar with a 30% replacement of re-fired and ground ash compared to the consumption of 12.07  $\text{kg}/\text{MPa}$  of the reference composite; thus, a reduction in clinker consumption of approximately 30% for the equivalent compressive strength was obtained.

For mortars with a fixed w/b factor in weight (Table 6), it is possible to observe that the lowest clinker consumption by compressive strength was 7.82  $\text{kg}/\text{MPa}$  for the mortar with a 30% replacement of burnt ash and ground compared to the consumption of 12.53  $\text{kg}/\text{MPa}$  of the reference mortar; thus, a reduction in clinker consumption of approximately 38% was obtained.

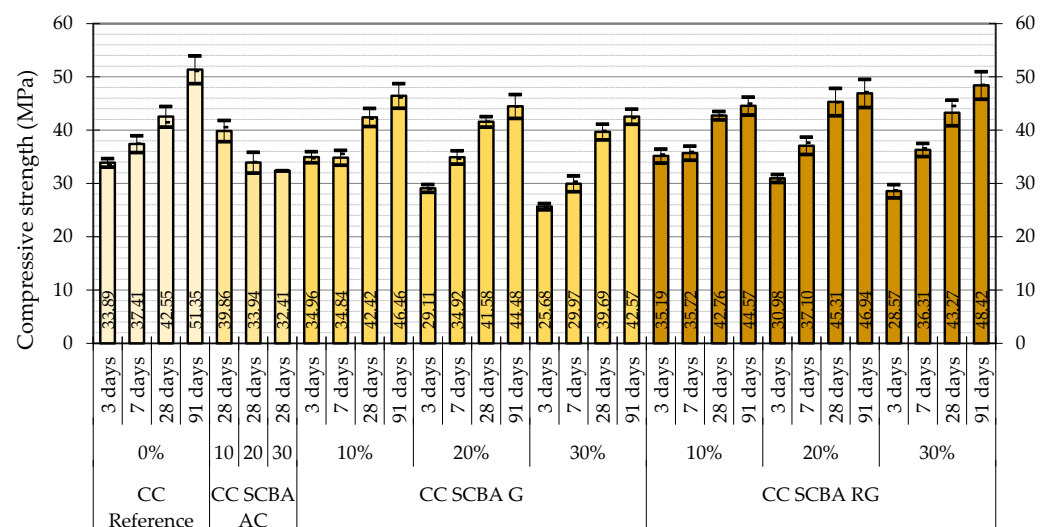


Figure 11. Compressive strength of mortars with a water/binder factor fixed in volume.

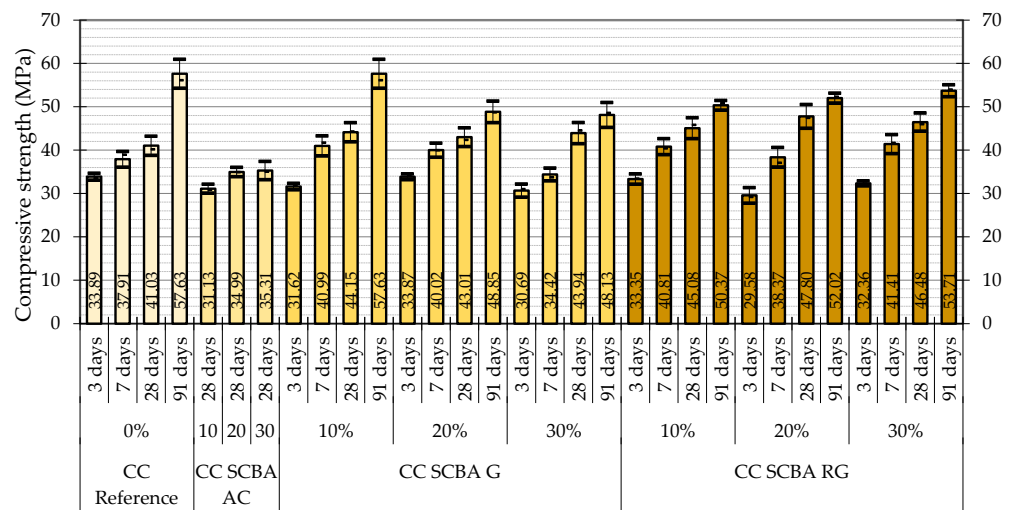


Figure 12. Compressive strength of mortars with a water/binder factor fixed in weight.

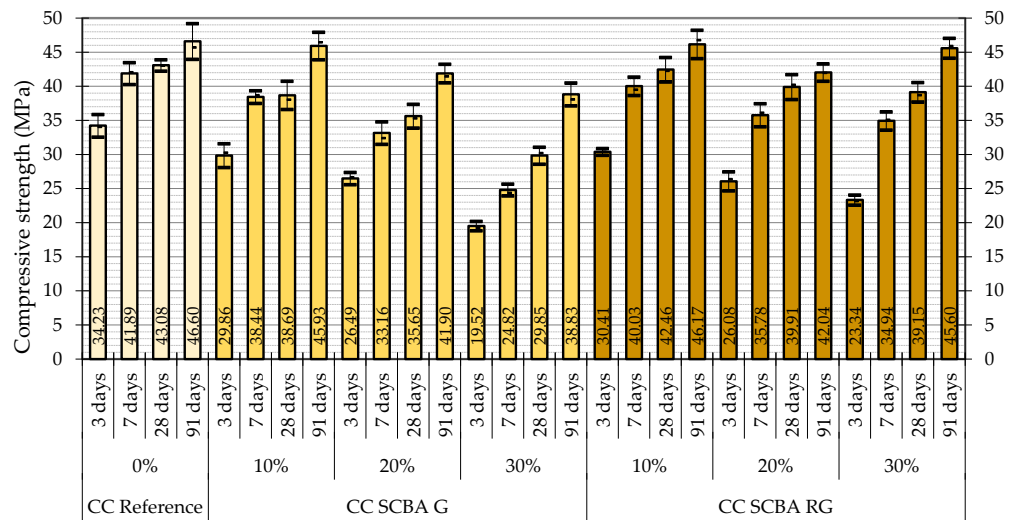


Figure 13. Compressive strength of mortars with the fixed flow.

Table 5. Comparisons between cement or binder consumption by compressive strength of mortars with fixed water/binder factor in volume.

Method	Mortar	Subst. (%)	Clinker Consumption per Volume (kg/m <sup>3</sup> )	SCBA Consumption per Volume (kg/m <sup>3</sup> )	Water/Binder in Volume	Water/Binder in Weight	Clinker Consumption per Strength (kg/MPa)	Binder Consumption per Strength (kg/MPa)
Water/binder factor fixed in volume	CC reference	0%	513.8	0.0	1.49	0.48	12.07	12.07
	CC SCBA AC	10%	462.4	28.5	1.49	0.50	11.60	12.31
		20%	411.0	56.9	1.49	0.53	12.11	13.79
		30%	359.6	85.4	1.49	0.56	11.10	13.73
		10%	462.4	32.7	1.49	0.50	10.90	11.67
	CC SCBA G	20%	411.0	65.4	1.49	0.52	9.89	11.46
		30%	359.6	98.1	1.49	0.54	9.06	11.53
	CC SCBA RG	10%	462.4	43.9	1.49	0.49	10.81	11.84
		20%	411.0	87.8	1.49	0.50	9.07	11.01
		30%	359.6	131.6	1.49	0.50	8.31	11.35

**Table 6.** Comparisons between cement or agglomerate consumption due to compression strength of mortars with water/binder factor fixed in weight.

Method	Mortar	Subst. (%)	Clinker Consumption per Volume (kg/m <sup>3</sup> )	SCBA Consumption per Volume (kg/m <sup>3</sup> )	Water/Binder in Volume	Water/Binder in Weight	Clinker Consumption per Strength (kg/MPa)	Binder Consumption per Strength (kg/MPa)
Water/binder factor fixed in weight	CC reference	0%	514.0	0.0	1.49	0.48	12.53	12.53
		10%	467.7	28.8	1.42	0.48	15.02	15.95
	CC SCBA AC	20%	420.4	58.2	1.36	0.48	12.02	13.68
		30%	372.0	88.3	1.29	0.48	10.54	13.04
	CC SCBA G	10%	466.8	33.0	1.44	0.48	10.57	11.32
		20%	418.7	66.6	1.38	0.48	9.73	11.28
		30%	369.7	100.9	1.33	0.48	8.41	10.71
	CC SCBA RG	10%	464.2	44.1	1.47	0.48	10.30	11.27
		20%	414.1	88.4	1.45	0.48	8.66	10.51
		30%	363.7	133.1	1.43	0.48	7.82	10.69

For mortars with the fixed flow (Table 7), it is possible to observe that the lowest clinker consumption by compressive strength was 8.77 kg/MPa for the mortar with a 30% replacement of re-fired and ground ash compared to the consumption of 11.68 kg/MPa of the reference mortar; thus, a reduction in clinker consumption of approximately 25% was obtained.

**Table 7.** Comparisons between cement or binder consumption due to the compressive strength of mortars with the fixed flow.

Method	Mortar	Subst. (%)	Clinker Consumption per Volume (kg/m <sup>3</sup> )	SCBA Consumption per Volume (kg/m <sup>3</sup> )	Water/Binder in Volume	Water/Binder in Weight	Clinker Consumption per Strength (kg/MPa)	Binder Consumption per Strength (kg/MPa)
Fixed flow	CC reference	0%	503.2	0.0	1.62	0.52	11.68	11.68
		10%	448.0	31.7	1.69	0.56	11.58	12.40
	CC SCBA G	20%	395.4	62.9	1.73	0.60	11.09	12.86
		30%	342.4	93.4	1.80	0.65	11.47	14.60
	CC SCBA RG	10%	447.5	42.5	1.70	0.55	10.54	11.54
		20%	394.3	84.2	1.75	0.58	9.88	11.99
		30%	343.4	125.7	1.78	0.60	8.77	11.98

Assessing the feasibility of replacing ground clinker with processed ashes in the economic context is essential. However, an analysis of the SCBA-based mixed Portland cement production life cycle, including the economic and environmental benefits, needs to be carried out to obtain SCBA acceptance in the cement industries [55]. The final cost of the Portland cement produced should lead to more accessible concrete. The main expense of SCBA is transportation; however, cement also has transport costs from the manufacturing site to the consumption site. The cost of grinding includes energy consumption, depreciation of equipment, and labor, and is approximately 30% of the total cost of SCBA. The cost of Portland cement calculated for Thailand was US\$ 64.7/ton against US\$ 15.0/ton for SCBA [77]. Chindaprasirt et al. [77] present CO<sub>2</sub>-eq emissions almost eight times lower for SCBA when compared to Portland cement.

Currently, SCBA is a residue from the sugar and alcohol industry without a high-added-value destination and is usually deposited in landfills, which does not add economic value. It is worth noting that the temperature of the thermal treatment of ash proposed in this work is about 40% of the manufacturing temperature of Portland cement. The

temperature of burning in thermoelectric plants and boilers is not controlled; however, having a commercial interest, it is believed that this temperature can be adjusted with some ease, which can eliminate the need for reprocessing by burning. Another important aspect is that the natural ash presents in granulometry and strength inferior to the limestone and Portland cement clinker, being easier to grind. These factors are likely to lead to burning and grinding costs lower than the cement manufacturing process costs.

The cost of ash was compared as a percentage to the cost of cement for mortars produced with a water/binder factor fixed in volume (Figure 14). For comparative purposes, the graph of the cost reduction with binder in the production of concrete versus the cost of ash in relation to cement was plotted, considering ash at zero cost (0%) or with the exact cost of cement (100%) and the binder consumption for the acquired strength (kg/MPa). Considering the results obtained, it can be said that, in terms of costs, the savings will be 9.69%, 18.06%, and 24.86% for the replacement of 10%, 20%, and 30% of cement by SCBA G at no acquisition cost, respectively. For the ash acquisition cost equal to that cost of cement (100%), the savings will still be 3.31%, 5.05%, and 4.47% for 10%, 20%, and 30% of substitutions, respectively. The cost breakeven point, that is, when the cost of Portland cement concrete will be the same as the cost of Portland cement concrete with ash, will happen when the value of the ground ash reaches 223.8%, 147.1%, and 121.8% for substitutions of 10%, 20%, and 30% of cement by SCBA G, respectively.

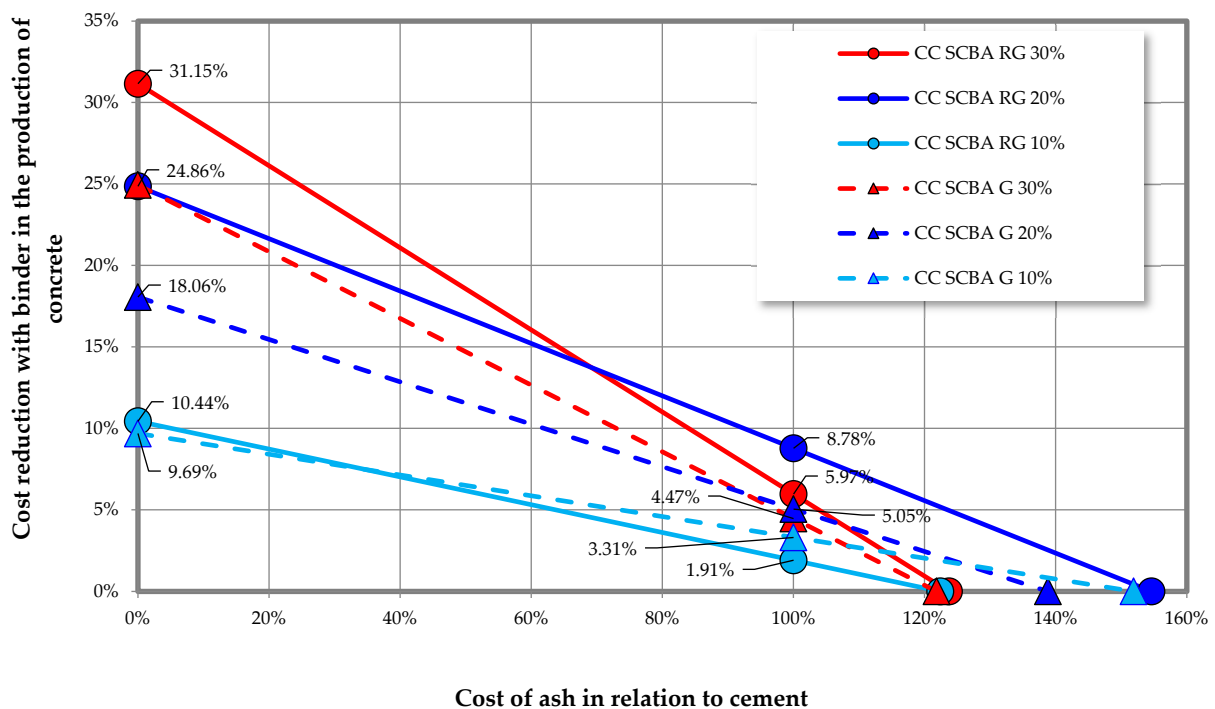


Figure 14. Mortar and concrete cost comparisons for SCBA relative cost variation.

For substitutions with re-fired and ground ash, the cost reduction will be 10.44% for concrete with a 10% replacement, 24.86% for 20%, and 31.15% for 30%. For the cost of ash equal to cement (100%), the savings will still be 1.91%, 8.78%, and 5.97% for 10, 20, and 30% of substitutions, respectively. The cost breakeven point will happen when the re-burnt and ground ash value reaches 122.4% of the cement value for 10%, 154.6% for 20%, and 123.7% for the 30% replacement, considering the same compressive strength acquired.

Therefore, taking into account that the cost of ash is around 23% of the cost of Portland cement and with emissions eight times lower [77], based on the data presented in Figure 14, there is financial and environmental viability in the use of SCBA for the production of mortars and concrete.

Another mechanical parameter evaluated was the flexural strength of mortars produced with SCBA G and SCBA RG, shown in Figure 15. Note that the tensile strengths of mortars with SCBA RG reached higher values than standard mortar. An analysis of the dry bulk density showed that the results were superior, and the results of water absorption were lower with the SCBA RG addition. These results correlated with better performance in the compressive and flexural strength of the mixtures with the addition of the SCBA RG, which was due to the filler action and the pozzolanic effect because the compressive and flexural strength has increased. The positive influence of the burning of sugar cane bagasse ash is confirmed in the literature [33].

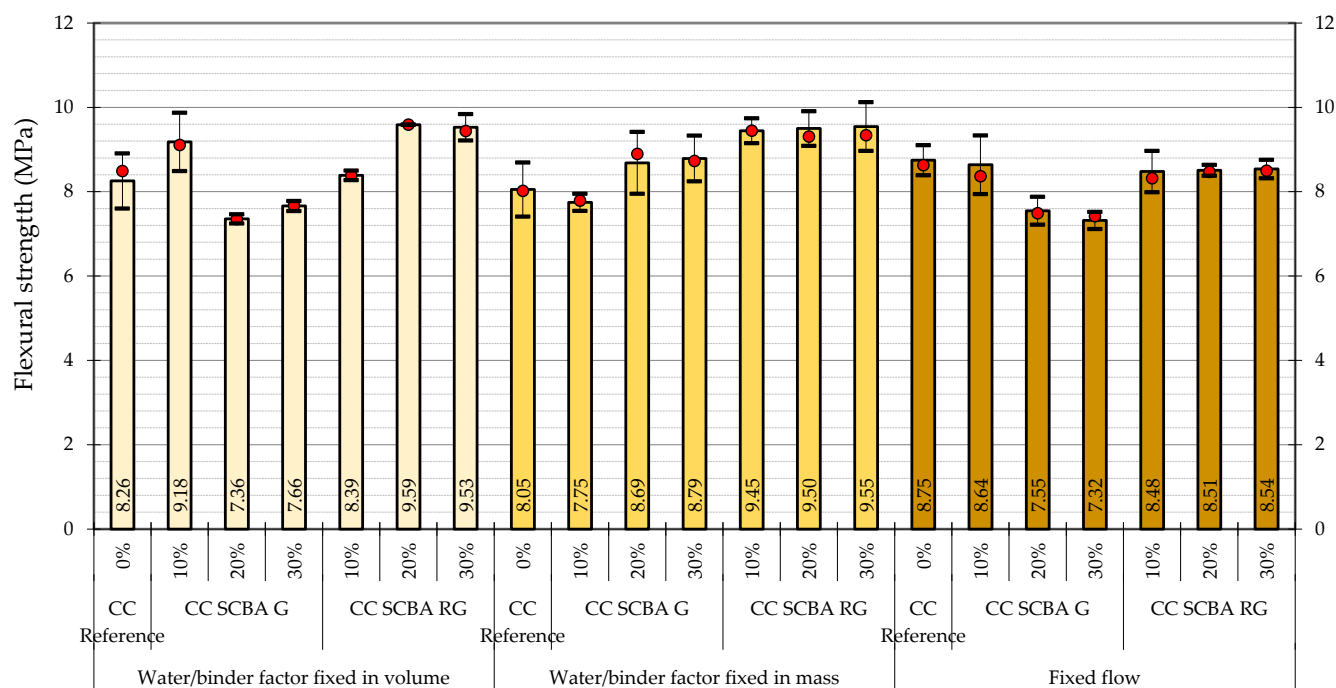


Figure 15. Flexural strength of mortars.

Regarding the potential of SCBA to inhibit harmful alkali–silica reactions, in Figures 16 and 17, it can be seen that SCBA RG presented an inhibition of the expansion of mortars higher than the inhibition of SCBA G. It has been found that the expansion was inverse to the content of SCBA for both SCBA G and SCBA RG. It is believed that the inhibition of expandability is related to two mechanisms of action. The first mechanism would be SCBA's performance as pozzolans, providing a greater cement alkali consumption, inhibiting the composites' expandability [78–80]. The second mechanism would be the SCBA's performance as a filler [81–83], providing the reduction of the composites' porosity through pore filling by SCBA G and SCBA RG, reducing the entry of water alkalis that are available in the sodium hydroxide solution. Both mechanisms justify the better performance of the SCBA RG since it has a smaller particle size and a higher amount of SiO<sub>2</sub>.

Flexural strength mortars with reactive aggregates before the ASR test is shown in Figure 18. The flexural tensile strength for mortars 900 days after the ASR expandability test is shown in Figure 19. You can see that the mortars with SCBA RG maintained higher levels of tensile strength in flexion after the alkalis attack. In general, the SCBA thermal treatment improves the performance of mortars in several aspects, as reported in the literature [30], including mechanically and in the inhibition of expansions caused by ASR.

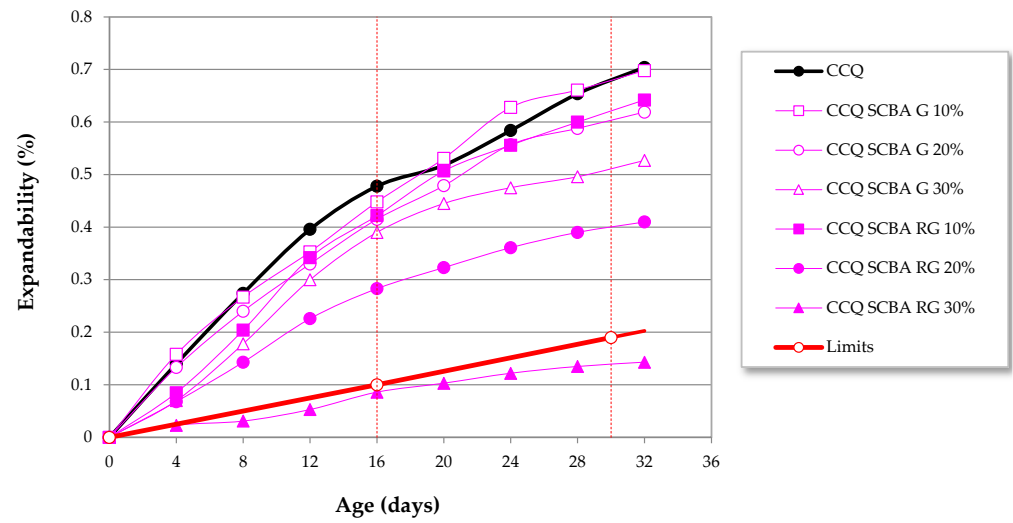


Figure 16. Comparison between the expandability of mortars developed with quartzite aggregates.

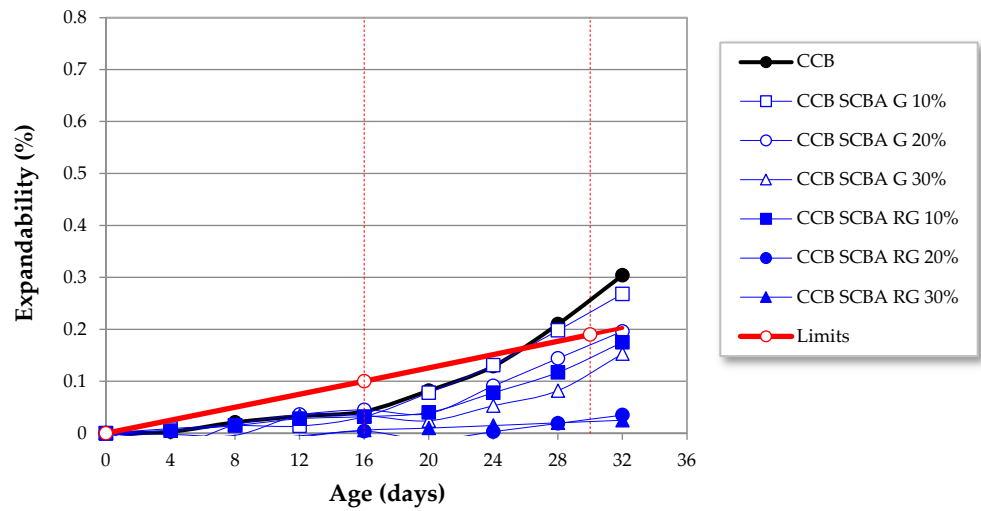


Figure 17. Comparison between the expandability of mortars developed with basalt aggregates.

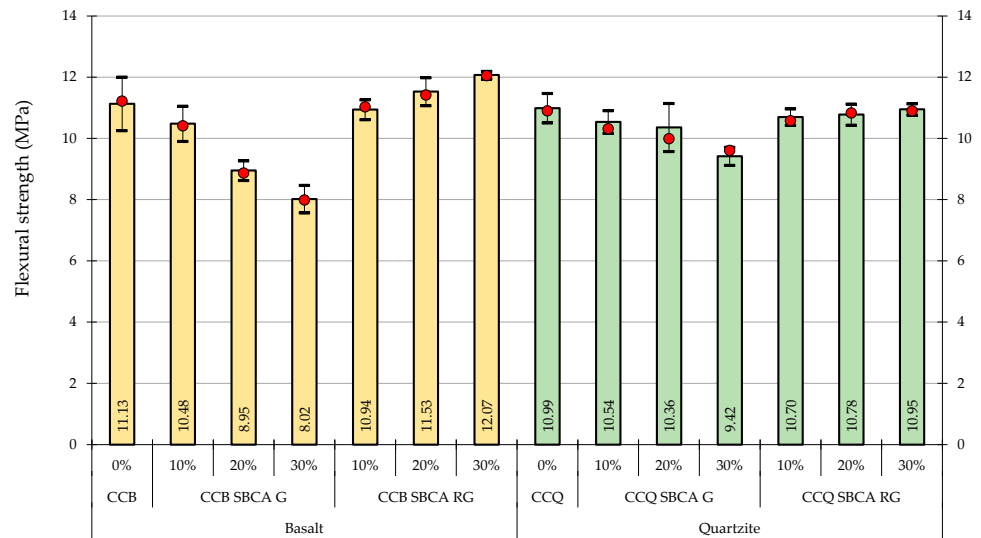


Figure 18. Flexural strength mortars with reactive aggregates before the ASR test.

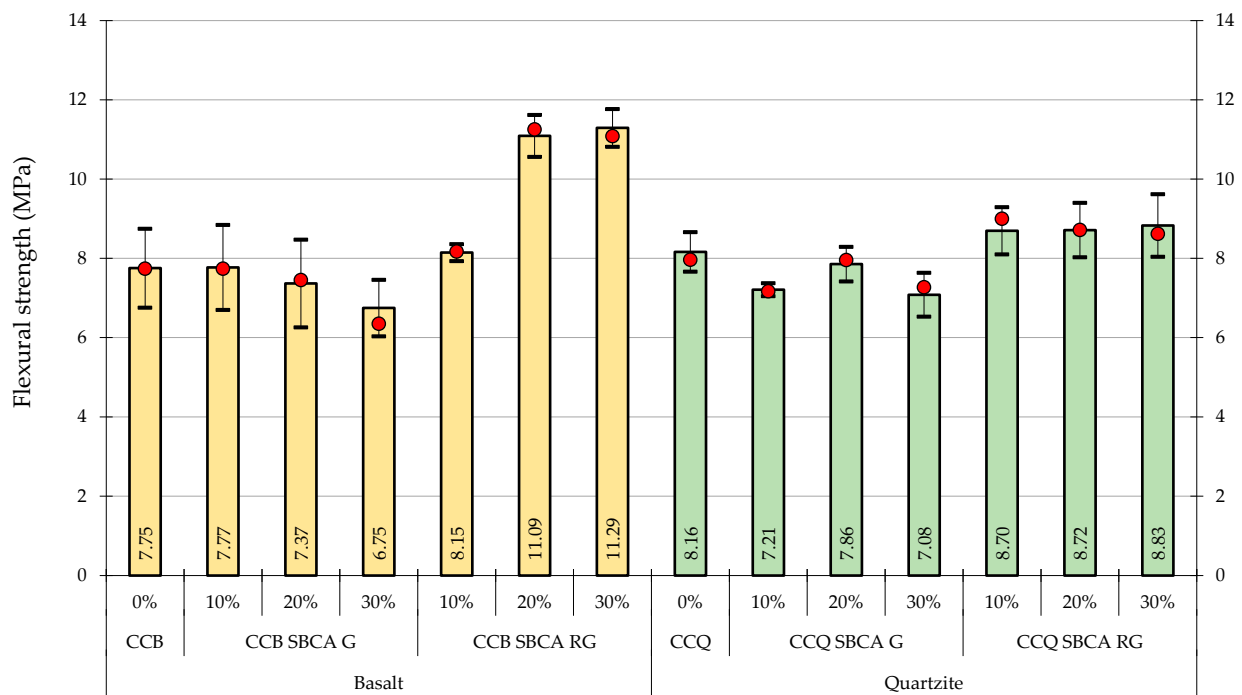


Figure 19. Flexural strength at 900 days of mortars after ASR test.

#### 4. Conclusions

This study demonstrated the possibility of using SCBA to produce Portland cement. The partial replacement of the Portland cement clinker by SCBA was feasible, and the conclusions below were made:

1. The processing of SCBA by grinding or burning promotes morphological and physical changes. Grinding and burning increased the density and reduced the particle size of SCBA. SCBA AC and SCBA G showed a high loss on ignition. SCBA G and SCBA RG are pozzolanic.
2. The cement produced with SCBA AC took the mortar with an inadequate consistency. The cement with SCBA G and SCBA RG did not have its setting time significantly altered. The higher percentage of additions (20% and 30%) of SCBA RG led to mortars with a higher dry bulk density and lower water absorption. The compressive strength of mortars with the cement with SCBA G and SCBA RG were compatible with the results obtained by the reference Portland cement, regardless of the dosage method used.
3. SCBA RG presented the lowest consumption of the Portland cement reference by compressive strength acquired in the dosing methods: (a) fixed water/binder factor in volume; (b) water/binder factor fixed in weight; and (c) fixed flow.
4. Without considering logistical costs, if SCBA's processing costs are zero, the savings in Portland cement production can reach 31.15%. For replacements of up to 30% of the clinker by SCBA, if the cost of the SCBA is equal to the cost of the clinker, the savings can reach 8.78%. It is worth noting that the temperature adjustment of the boilers of the thermoelectric plants can lead to SCBA being more suitable for the partial replacement of the clinker, without the need for re-firing, and the grinding of the SCBA requires less energy than the grinding of the clinker, mainly due to the size of the SGBA AC being reduced compared to the clinker.
5. The clinker's replacement by SCBA reduces the expansion of mortar prisms with reactive aggregates exposed to aggressive environments (NaOH solution at 80 °C for 28 days). The SCBA RG in the 30% Portland clinker substitution inhibits expansion by ASR with the used aggregates of quartzite and basalt. This fact is confirmed by the flexural strength presented by CC SCBA RG 30% after 900 days of the ASR test.

In addition to reducing the Portland cement clinker caused by the use of SCBA, the incorporation of SCBA G and SCBA RG imprisons 49.2% and 3.3% of the material content with incomplete combustion rich in carbon in the matrix. This incorporation did not significantly change the setting time, porosity, and durability at ASR of the matrix produced. This subject should be researched with the intent of proving carbon capture.

**Author Contributions:** Conceptualization, M.C.N.F.F. and A.C.d.S.B.; methodology, M.C.N.F.F. and A.C.d.S.B.; validation, R.C.G., M.C.N.F.F. and A.C.d.S.B.; formal analysis, R.C.G., M.C.N.F.F., C.d.S.R., M.T.P.A. and A.C.d.S.B.; investigation, S.L.C.S. and A.C.d.S.B.; resources, M.V.d.M.S.S. and A.C.d.S.B.; data curation, R.C.G. and A.C.d.S.B.; writing—original draft preparation, S.L.C.S., S.F., L.N.S. and A.C.d.S.B.; writing—review and editing, S.F., L.N.S. and A.C.d.S.B.; visualization, S.F., L.N.S. and A.C.d.S.B.; supervision, R.C.G. and A.C.d.S.B.; project administration, M.V.d.M.S.S. and A.C.d.S.B.; funding acquisition, A.C.d.S.B. All authors have read and agreed to the published version of the manuscript.

**Funding:** This work was supported by the Energy Company of Minas Gerais (CEMIG) and the National Electric Energy Agency (ANEEL) for funding through the PD ANEEL CEMIG GT331 and PD ANEEL CEMIG GT616 projects, the Minas Gerais State Research Foundation (FAPEMIG) [grant number APQ-03739-16] for their assistance with the infrastructure, and National Council for Scientific and Technological Development (CNPq) [grant number PQ 315653/2020-5] for the research productivity incentive grant.

**Institutional Review Board Statement:** Not applicable.

**Informed Consent Statement:** Not applicable.

**Data Availability Statement:** The data presented in this study are available upon request from the corresponding author.

**Conflicts of Interest:** The authors declare no competing financial interests or personal relationships that could appear to influence the work reported in this paper.

## References

1. Scrivener, K.L.; John, V.M.; Gartner, E.M. Eco-efficient cements: Potential economically viable solutions for a low-CO<sub>2</sub> cement-based materials industry. *Cem. Concr. Res.* **2018**, *114*, 2–26. [[CrossRef](#)]
2. United States Geological Survey. *Mineral Commodity Summaries 2022*; United States Geological Survey: Reston, VA, USA, 2022.
3. Ali, N.; Mohd Sobri, M.H.A.; Hadipramana, J.; Abdul Samad, A.A.; Mohamad, N. Potential Mixture of POFA and SCBA as Cement Replacement in Concrete—A Review. *MATEC Web Conf.* **2017**, *103*, 01006. [[CrossRef](#)]
4. Paris, J.M.; Roessler, J.G.; Ferraro, C.C.; Deford, H.D.; Townsend, T.G. A review of waste products utilized as supplements to Portland cement in concrete. *J. Clean. Prod.* **2016**, *121*, 1–18. [[CrossRef](#)]
5. Lorena Figueiredo Martins, M.; Roberto Ribeiro Soares Junior, P.; Henrique da Silva, T.; de Souza Maciel, P.; Peixoto Pinheiro, I.; Cesar da Silva Bezerra, A. Magnesium industry waste and red mud to eco-friendly ternary binder: Producing more sustainable cementitious materials. *Constr. Build. Mater.* **2021**, *310*, 125172. [[CrossRef](#)]
6. Gołaszewski, J.; Gołaszewska, M.; Cygan, G. Performance of Ordinary and Self-Compacting Concrete with Limestone after Freeze–Thaw Cycles. *Buildings* **2022**, *12*, 2003. [[CrossRef](#)]
7. Khatib, J.; Ramadan, R.; Ghanem, H.; Elkordi, A. Volume stability of cement paste containing limestone fines. *Buildings* **2021**, *11*, 366. [[CrossRef](#)]
8. Choi, Y.C.; Park, B. Enhanced autogenous healing of ground granulated blast furnace slag blended cements and mortars. *J. Mater. Res. Technol.* **2019**, *8*, 3443–3452. [[CrossRef](#)]
9. Ramakrishnan, K.; Pugazhmani, G.; Sripragadeesh, R.; Muthu, D.; Venkatasubramanian, C. Experimental study on the mechanical and durability properties of concrete with waste glass powder and ground granulated blast furnace slag as supplementary cementitious materials. *Constr. Build. Mater.* **2017**, *156*, 739–749. [[CrossRef](#)]
10. Zeraoui, A.; Maherzi, W.; Benzerzour, M.; Abriak, N.E.; Aouad, G. Development of Flash—Calcined Sediment and Blast Furnace Slag Ternary Binders. *Buildings* **2023**, *13*, 333. [[CrossRef](#)]
11. Ramzi, S.; Hajiloo, H. The Effects of Supplementary Cementitious Materials (SCMs) on the Residual Mechanical Properties of Concrete after Exposure to High Temperatures—Review. *Buildings* **2022**, *13*, 103. [[CrossRef](#)]
12. Barboza-Chavez, A.C.; Gómez-Zamorano, L.Y.; Acevedo-Dávila, J.L. Synthesis and characterization of a hybrid cement based on fly ash, metakaolin and portland cement clinker. *Materials* **2020**, *13*, 1084. [[CrossRef](#)] [[PubMed](#)]
13. Ahmad, J.; Majdi, A.; Arbili, M.M.; Deifalla, A.F.; Naqash, M.T. Mechanical, Durability and Microstructure Analysis Overview of Concrete Made with Metakaolin (MTK). *Buildings* **2022**, *12*, 1401. [[CrossRef](#)]

14. Yanez, S.; Márquez, C.; Valenzuela, B.; Villamar-Ayala, C.A. A Bibliometric-Statistical Review of Organic Residues as Cementitious Building Materials. *Buildings* **2022**, *12*, 597. [[CrossRef](#)]
15. Young, G.; Yang, M. Preparation and characterization of Portland cement clinker from iron ore tailings. *Constr. Build. Mater.* **2019**, *197*, 152–156. [[CrossRef](#)]
16. Gou, M.; Zhou, L.; Then, N.W.Y. Utilization of tailings in cement and concrete: A review. *Sci. Eng. Compos. Mater.* **2019**, *26*, 449–464. [[CrossRef](#)]
17. Magalhães, L.F.D.; França, S.; Oliveira, M.D.S.; Peixoto, R.A.F.; Bessa, S.A.L.; Bezerra, A.C.D.S. Iron ore tailings as a supplementary cementitious material in the production of pigmented cements. *J. Clean. Prod.* **2020**, *274*, 123260. [[CrossRef](#)]
18. ABNT NBR 16697; Cimento Portland—Requisitos. Associação Brasileira de Normas Técnicas (ABNT): São Paulo, Brazil, 2018.
19. Teixeira, A.H.C.; Junior, P.R.R.S.; Silva, T.H.; Barreto, R.R.; da Silva Bezerra, A.C. Low-carbon concrete based on binary biomass ash-silica fume binder to produce eco-friendly paving blocks. *Materials* **2020**, *13*, 1534. [[CrossRef](#)]
20. Gutiérrez-Orrego, D.A.; Gómez-Botero, M.A.; García, E.F. Alkali-Activated Hybrid Cement from Mineral Wool Fiber Waste and OPC. *Buildings* **2023**, *13*, 354. [[CrossRef](#)]
21. De Matos Neto, J.A.; De Resende, D.S.; Da Silva Neto, J.T.; De Gouveia, A.M.C.; De Aguiar, M.T.P.; Da Silva Bezerra, A.C. Sterile clay pozzolans from phosphate mining. *Mater. Res.* **2015**, *18*, 230–234. [[CrossRef](#)]
22. Li, J.; Ren, W.; Zhang, A.; Li, S.; Tan, J.; Liu, H. Mechanical Properties and Microstructure Analysis of Cement Mortar Mixed with Iron Ore Tailings. *Buildings* **2023**, *13*, 149. [[CrossRef](#)]
23. Kim, J.; Lee, D.; Sičáková, A.; Kim, N. Utilization of Different Forms of Demolished Clay Brick and Granite Wastes for Better Performance in Cement Composites. *Buildings* **2023**, *13*, 165. [[CrossRef](#)]
24. de Magalhães, L.F.; de Souza Morais, I.; Lara, L.F.D.S.; de Resende, D.S.; Menezes, R.M.R.O.; Aguiar, M.T.P.; da Silva Bezerra, A.C. Iron ore tailing as addition to partial replacement of portland cement. *Mater. Sci. Forum* **2018**, *930*, 125–130. [[CrossRef](#)]
25. de Souza Morais, I.; de Magalhães, L.F.; Lara, L.F.D.S.; Corrêa, E.C.S.; Menezes, R.M.R.O.; Aguiar, M.T.P.; da Silva Bezerra, A.C. Sericitic phyllite as addition in portland cement. *Mater. Sci. Forum* **2018**, *930*, 131–136. [[CrossRef](#)]
26. Ye, J.; Liu, S.; Zhao, Y.; Li, Y.; Fang, J.; Zhang, H.; Guan, X. Development of Ultrafine Mineral Admixture from Magnesium Slag and Sequestration of CO<sub>2</sub>. *Buildings* **2023**, *13*, 204. [[CrossRef](#)]
27. Duarte, M.S.; Almada, B.S.; José dos Santos, W.; Lima Bessa, S.A.; Cesar da Silva Bezerra, A.; Paulino Aguiar, M.T. Influence of mechanical treatment and magnetic separation on the performance of iron ore tailings as supplementary cementitious material. *J. Build. Eng.* **2022**, *59*, 105099. [[CrossRef](#)]
28. Pires, M.; de Jesus Andrade Fidelis, R.; de Resende, D.S.; da Silva Bezerra, A.C. Phosphate rock waste in the production of cement tile. *Results Eng.* **2022**, *16*, 100701. [[CrossRef](#)]
29. OECD/FAO. *OECD-FAO Agricultural Outlook 2020–2029*; OECD/FAO: Paris, France, 2020; ISBN 9789264317673.
30. da Silva Bezerra, A.C.; Saraiva, S.L.C.; dos Silva Lara, L.F.; de Castro, L.W.A.; Gomes, R.C.; de Silva Rodrigues, C.; Ferreira, M.C.N.F.; Aguiar, M.T.P. Effect of partial replacement with thermally processed sugar cane bagasse on the properties of mortars. *Rev. Mater.* **2017**, *22*, e11785. [[CrossRef](#)]
31. Rezende, M.F.; Machado, F.C.S.; Gouveia, A.M.C.; Bezerra, A.C.S.; Grillo, R.H.F.; Ortigara, Y.V.B. Substituição parcial do cimento Portland pela cinza de bagaço de cana-de-açúcar em habitações de interesse social. *Rev. Agrogeoambiental* **2017**, *9*, 1. [[CrossRef](#)]
32. Soares, M.M.N.S.; Poggiali, F.S.J.; Bezerra, A.C.S.; Figueiredo, R.B.; Aguiar, M.T.P.; Cetlin, P.R. The effect of calcination conditions on the physical and chemical characteristics of sugar cane bagasse ash. *Rem. Rev. Esc. Minas* **2014**, *67*, 33–39. [[CrossRef](#)]
33. Ferreira, R.T.L.; Nunes, F.M.M.P.; Bezerra, A.C.S.; Figueiredo, R.B.; Cetlin, P.R.; Aguiar, M.T.P. Influence of reburning on the pozzolonicity of sugar-cane bagasse ashes with different characteristics. *Mater. Sci. Forum* **2016**, *869*, 141–146. [[CrossRef](#)]
34. Mohan, R.; Athira, G.; Mali, A.K.; Bahurudeen, A.; Nanthagopalan, P. Systematic Pretreatment Process and Optimization of Sugarcane Bagasse Ash Dosage for Use in Cement-Based Products. *J. Mater. Civ. Eng.* **2021**, *33*, 04021045. [[CrossRef](#)]
35. Sousa, L.N.; Figueiredo, P.F.; França, S.; de Moura Solar Silva, M.V.; Borges, P.H.R.; da Silva Bezerra, A.C. Effect of Non-Calcined Sugarcane Bagasse Ash as an Alternative Precursor on the Properties of Alkali-Activated Pastes. *Molecules* **2022**, *27*, 1185. [[CrossRef](#)] [[PubMed](#)]
36. Silva, T.H.; Lara, L.F.S.; Silva, G.J.B.; Provis, J.L.; Bezerra, A.C.S. Alkali-activated materials produced using high-calcium, high-carbon biomass ash. *Cem. Concr. Compos.* **2022**, *132*, 104646. [[CrossRef](#)]
37. Cordeiro, G.C.; Toledo Filho, R.D.; Fairbairn, E.M.R. Effect of calcination temperature on the pozzolanic activity of sugar cane bagasse ash. *Constr. Build. Mater.* **2009**, *23*, 3301–3303. [[CrossRef](#)]
38. ASTM C618-19; Standard Specification for Coal Fly Ash and Raw or Calcined Natural Pozzolan for Use in Concrete. ASTM International: West Conshohocken, PA, USA, 2019.
39. ABNT NBR 5752; Materiais Pozolânicos—Determinação do Índice Desempenho com Cimento Portland aos 28 Dias. Associação Brasileira de Normas Técnicas: São Paulo, Brazil, 2014.
40. ABNT NBR 15895; Materiais Pozolânicos—Determinação do Teor de Hidróxido de Cálcio Fixado—Método Chapelle Modificado. Associação Brasileira de Normas Técnicas: São Paulo, Brazil, 2010.
41. Moreira, M.A.N.S.; Heitmann, A.P.; Bezerra, A.C.S.; Patrício, P.S.O.; de Oliveira, L.C.A.; Castro, C.S.; de Souza, P.P. Photocatalytic performance of cementitious materials with addition of red mud and Nb<sub>2</sub>O<sub>5</sub> particles. *Constr. Build. Mater.* **2020**, *259*, 119851. [[CrossRef](#)]

42. Silva, T.H.; Castro, A.C.M.; Valente Neto, F.C.; Soares, M.M.N.S.; De Resende, D.S.; Bezerra, A.C.S. Recycling ceramic waste as a raw material in sanitary ware production. *Ceramica* **2019**, *65*, 426–431. [[CrossRef](#)]
43. Moraes, C.F.; Belo, B.R.; Bezerra, A.C.S.; Loura, R.M.; Porto, M.P.; Bessa, S.A.L. Thermal and mechanical analyses of colored mortars produced using Brazilian iron ore tailings. *Constr. Build. Mater.* **2021**, *268*, 121073. [[CrossRef](#)]
44. ABNT NM 65; Cimento Portland—Determinação dos Tempos de Pega. Associação Brasileira de Normas Técnicas: São Paulo, Brazil, 2003.
45. ABNT NBR 7215; Cimento Portland—Determinação da Resistência à Compressão de Corpos de Prova Cilíndricos. Associação Brasileira de Normas Técnicas: São Paulo, Brazil, 2019.
46. ABNT NBR 7214; Areia Normal para Ensaio de Cimento (Especificação). Associação Brasileira de Normas Técnicas: São Paulo, Brazil, 2015.
47. EN 197-1; Cement—Part 1: Composition, Specifications and Conformity Criteria for Common Cements. European Committee for Standardization: Brussels, Belgium, 2000.
48. ABNT NBR 13279; Argamassa para Assentamento e Revestimento de Paredes e Tetos—Determinação da Resistência à Tração na Flexão e à Compressão. Associação Brasileira de Normas Técnicas: São Paulo, Brazil, 2005.
49. ABNT NBR 9778; Argamassa e Concreto Endurecidos—Determinação da Absorção de Água, Índice de Vazios E Massa Específica. Associação Brasileira de Normas Técnicas: São Paulo, Brazil, 2005.
50. ASTM International (2014) C 1260-14; Standard Test Method Potential Alkali React. Aggregates (Mortar-Bar Method). ASTM International: West Conshohocken, PA, USA, 2014.
51. ABNT NBR 15577-5; Agregados—Reatividade Álcali-Agregado Parte 5: Determinação da Mitigação da Expansão em Barras de Argamassa pelo Método Acelerado. Associação Brasileira de Normas Técnicas: São Paulo, Brazil, 2018.
52. ABNT NNBR 15577-4; Agregados—Reatividade Álcali-Agregado Parte 4: Determinação da Expansão em Barras de Argamassa pelo Método Acelerado. Associação Brasileira de Normas Técnicas: São Paulo, Brazil, 2018; ISBN 978-85-07-07583-7.
53. Deepika, S.; Anand, G.; Bahurudeen, A.; Santhanam, M. Construction Products with Sugarcane Bagasse Ash Binder. *J. Mater. Civ. Eng.* **2017**, *29*, 04017189. [[CrossRef](#)]
54. Athira, V.S.; Charitha, V.; Athira, G.; Bahurudeen, A. Agro-waste ash based alkali-activated binder: Cleaner production of zero cement concrete for construction. *J. Clean. Prod.* **2021**, *286*, 125429. [[CrossRef](#)]
55. Jittin, V.; Minnu, S.N.; Bahurudeen, A. Potential of sugarcane bagasse ash as supplementary cementitious material and comparison with currently used rice husk ash. *Constr. Build. Mater.* **2020**, *273*, 121679. [[CrossRef](#)]
56. Yadav, A.L.; Sairam, V.; Srinivasan, K.; Muruganandam, L. Synthesis and characterization of geopolymer from metakaolin and sugarcane bagasse ash. *Constr. Build. Mater.* **2020**, *258*, 119231. [[CrossRef](#)]
57. Akbar, A.; Farooq, F.; Shafique, M.; Aslam, F.; Alyousef, R.; Alabduljabbar, H. Sugarcane bagasse ash-based engineered geopolymer mortar incorporating propylene fibers. *J. Build. Eng.* **2021**, *33*, 101492. [[CrossRef](#)]
58. Minnu, S.N.; Bahurudeen, A.; Athira, G. Comparison of sugarcane bagasse ash with fly ash and slag: An approach towards industrial acceptance of sugar industry waste in cleaner production of cement. *J. Clean. Prod.* **2021**, *285*, 124836. [[CrossRef](#)]
59. Moraes, J.C.B.; Cordeiro, G.C.; Akasaki, J.L.; Vieira, A.P.; Payá, J. Improving the reactivity of a former ground sugarcane bagasse ash produced by autogenous combustion through employment of two different additional grinding procedures. *Constr. Build. Mater.* **2021**, *270*, 121471. [[CrossRef](#)]
60. Lyra, G.P.; Borrachero, M.V.; Soriano, L.; Payá, J.; Rossignolo, J.A. Comparison of original and washed pure sugar cane bagasse ashes as supplementary cementing materials. *Constr. Build. Mater.* **2021**, *272*, 122001. [[CrossRef](#)]
61. Klathae, T.; Tanawuttiiphong, N.; Tangchirapat, W.; Chindaprasirt, P.; Sukontasukkul, P.; Jaturapitakkul, C. Heat evolution, strengths, and drying shrinkage of concrete containing high volume ground bagasse ash with different LOIs. *Constr. Build. Mater.* **2020**, *258*, 119443. [[CrossRef](#)]
62. Tavares, L.R.C.; Junior, J.F.T.; Costa, L.M.; da Silva Bezerra, A.C.; Cetlin, P.R.; Aguilar, M.T.P. Influence of quartz powder and silica fume on the performance of Portland cement. *Sci. Rep.* **2020**, *10*, 21461. [[CrossRef](#)]
63. ABNT NBR 12653; Materiais pozolânicos—Requisitos. Associação Brasileira de Normas Técnicas: São Paulo, Brazil, 2014.
64. Cordeiro, G.C.; Barroso, T.R.; Toledo Filho, R.D. Enhancement the Properties of Sugar Cane Bagasse Ash with High Carbon Content by a Controlled Re-calcination Process. *KSCE J. Civ. Eng.* **2018**, *22*, 1250–1257. [[CrossRef](#)]
65. Antao, S.M.; Hassan, I.; Wang, J.; Lee, P.L.; Toby, B.H. State-of-the-art high-resolution powder X-ray diffraction (HRPXRD) illustrated with rietveld structure refinement of quartz, sodalite, tremolite, and meionite. *Can. Mineral.* **2008**, *46*, 1501–1509. [[CrossRef](#)]
66. Dan’ko, A.J.; Rom, M.A.; Sidelnikova, N.S.; Nizhankovskiy, S.V.; Budnikov, A.T.; Grin, L.A.; Kaltaev, K.S.O. Transformation of the corundum structure upon high-temperature reduction. *Crystallogr. Rep.* **2008**, *53*, 1112–1118. [[CrossRef](#)]
67. Pauling, L.; Hendricks, S.B. The crystal structures of hematite and corundum. *J. Am. Chem. Soc.* **1925**, *47*, 781–790. [[CrossRef](#)]
68. Andreão, P.V.; Suleiman, A.R.; Cordeiro, G.C.; Nehdi, M.L. Beneficiation of Sugarcane Bagasse Ash: Pozzolanic Activity and Leaching Behavior. *Waste Biomass Valorization* **2020**, *11*, 4393–4402. [[CrossRef](#)]
69. Martins Torres, S.; Estolano de Lima, V.; de Azevedo Basto, P.; de Araújo Júnior, N.T.; de Melo Neto, A.A. Assessing the pozzolanic activity of sugarcane bagasse ash using X-ray diffraction. *Constr. Build. Mater.* **2020**, *264*, 120684. [[CrossRef](#)]
70. Figueiredo, R.L.; Pavia, S. A study of the parameters that determine the reactivity of sugarcane bagasse ashes (SCBA) for use as a binder in construction. *SN Appl. Sci.* **2020**, *2*, 1515. [[CrossRef](#)]

71. Katare, V.D.; Madurwar, M.V. Use of processed biomass ash as a sustainable pozzolana. *Curr. Sci.* **2019**, *116*, 741–750. [[CrossRef](#)]
72. Praveenkumar, S.; Sankarasubramanian, G. Synergic Effect of Sugarcane Bagasse Ash Based Cement on High Performance Concrete Properties. *Silicon* **2021**, *13*, 2357–2367. [[CrossRef](#)]
73. Bonfim, W.B.; de Paula, H.M. Characterization of different biomass ashes as supplementary cementitious material to produce coating mortar. *J. Clean. Prod.* **2021**, *291*, 125869. [[CrossRef](#)]
74. Raverdy, M.; Brivot, F.; Paillère, A.M.; Dron, R. Assessment of the pozzolanic activity of the secondary constituents (in French: Appreciation de l'activité pouzzolanique des constituants secondaires). In Proceedings of the 7th International Congress on the Chemistry of Cement, Paris, France, 1 January 1980; Volume 3, pp. 36–41.
75. Jahanzaib Khalil, M.; Aslam, M.; Ahmad, S. Utilization of sugarcane bagasse ash as cement replacement for the production of sustainable concrete—A review. *Constr. Build. Mater.* **2021**, *270*, 121371. [[CrossRef](#)]
76. Barbosa, F.L.; Cordeiro, G.C. Partial cement replacement by different sugar cane bagasse ashes: Hydration-related properties, compressive strength and autogenous shrinkage. *Constr. Build. Mater.* **2021**, *272*, 8–11. [[CrossRef](#)]
77. Chindaprasirt, P.; Kroehong, W.; Damrongwiriyanupap, N.; Suriyo, W.; Jaturapitakkul, C. Mechanical properties, chloride resistance and microstructure of Portland fly ash cement concrete containing high volume bagasse ash. *J. Build. Eng.* **2020**, *31*, 101415. [[CrossRef](#)]
78. da Silva Andrade Neto, J.; de França, M.J.S.; de Amorim Júnior, N.S.; Ribeiro, D.V. Effects of adding sugarcane bagasse ash on the properties and durability of concrete. *Constr. Build. Mater.* **2021**, *266*, 120959. [[CrossRef](#)]
79. Kazmi, S.M.S.; Munir, M.J.; Patnaikuni, I.; Wu, Y.F. Pozzolanic reaction of sugarcane bagasse ash and its role in controlling alkali silica reaction. *Constr. Build. Mater.* **2017**, *148*, 231–240. [[CrossRef](#)]
80. Abbas, S.; Sharif, A.; Ahmed, A.; Abbass, W.; Shaukat, S. Prospective of sugarcane bagasse ash for controlling the alkali-silica reaction in concrete incorporating reactive aggregates. *Struct. Concr.* **2020**, *21*, 781–793. [[CrossRef](#)]
81. Cordeiro, G.C.; Toledo Filho, R.D.; Tavares, L.M.; Fairbairn, E.M.R. Pozzolanic activity and filler effect of sugar cane bagasse ash in Portland cement and lime mortars. *Cem. Concr. Compos.* **2008**, *30*, 410–418. [[CrossRef](#)]
82. Cordeiro, G.C.; Tavares, L.M.; Toledo Filho, R.D. Improved pozzolanic activity of sugar cane bagasse ash by selective grinding and classification. *Cem. Concr. Res.* **2016**, *89*, 269–275. [[CrossRef](#)]
83. Zareei, S.A.; Ameri, F.; Bahrami, N. Microstructure, strength, and durability of eco-friendly concretes containing sugarcane bagasse ash. *Constr. Build. Mater.* **2018**, *184*, 258–268. [[CrossRef](#)]

**Disclaimer/Publisher's Note:** The statements, opinions and data contained in all publications are solely those of the individual author(s) and contributor(s) and not of MDPI and/or the editor(s). MDPI and/or the editor(s) disclaim responsibility for any injury to people or property resulting from any ideas, methods, instructions or products referred to in the content.